Synchronization universality classes and stability of smooth coupled map lattices

Franco Bagnoli[1,2,3] and Raúl Rechtman[4]

[1]*Dipartimento di Energetica, Università di Firenze, Via S. Marta 3, I–50139 Firenze, Italy*
[2]*Centro Interdipartimentale per lo Studio delle Dinamiche Complesse, Firenze, Italy*
[3]*INFN Sezione di Firenze, Firenze, Italy*
[4]*Centro de Investigación en Energía, Universidad Nacional Autónoma de México, Apdo. Postal 34 Temixco, Morelos 62580, Mexico*

We study two problems related to spatially extended systems: the dynamical stability and the universality classes of the replica synchronization transition. We use a simple model of one-dimensional coupled map lattices and show that chaotic behavior implies that the synchronization transition belongs to the multiplicative noise universality class, while stable chaos implies that the synchronization transition belongs to the directed percolation universality class.

I. INTRODUCTION

Chaos is a widely studied phenomenon. It represents the generic behavior of nonlinear systems and it is also assumed to be *the* microscopic mechanism for the amplification of uncertainties about initial conditions. The exponential growth of an initial small uncertainty is measured by the maximum Lyapunov exponent (MLE). However, in high-dimensional systems, and especially in extended systems with short-range coupling, the origin of uncertainty may be different from the previous one. To be more specific, the systems we take into considerations are defined on a lattice with short-range interactions.

Just to give a simple example of the different role of chaos in low-dimensional with respect to extended systems, let us consider an array of *uncoupled* chaotic maps. This is clearly a chaotic system; a localized uncertainty will grow in time and will remain localized. If there is a coupling between neighboring maps, a localized uncertainty will propagate to neighboring sites. This propagation is a linear phenomenon, and is hidden by the exponential amplification due to the chaotic dynamics of maps. If we now consider *nonchaotic* (i.e., stable) coupled maps, only the spreading mechanism may be present. Since the individual maps are stable, infinitesimal uncertainties are always absorbed, but *finite* ones may survive. One of the most striking examples are *class-3* cellular automata (CA) [1], that are equivalent to superstable maps, but may nevertheless be denoted "chaotic" because a localized uncertainty may spread to the whole system.

While cellular automata may be seen as coupled maps of extreme type, that only take values 0 and 1, CA-like behavior has been observed also in continuous maps, albeit with discontinuities or extremely sharp transitions [2]. In these cases the maximum Lyapunov exponent (if defined) is negative but defects and information may propagate and amplify in a nonexponential way. When finite, these systems are generally periodic, but the period grows at least exponentially with the size, so that the transient is the only observable state [2–4]. This behavior is denoted as *stable chaos*.

As mentioned before, evaluation of the MLE is the most direct method to establish the stability properties of a system but is somewhat limited for extended systems as coupled map lattices (CMLs). An alternative method for the measurement of uncertainty is based on the synchronization of replicas of a system [5,6]. Typically, one fraction of each replica is added to the other and the distance between them vanishes as this fraction varies [7,8]. Another mechanism involves the addition of the same external noise to both replicas [9]. In both cases, there is a control parameter *p* that measures the *strength* of the synchronization.

We may have different scenarios, according to the degree of unpredictability of the system. Chaotic systems are expected to amplify the distance between replicas. For a value of *p* slightly below the synchronization threshold, some patches may synchronize for some time, after which they will separate. This picture resembles that of a growing interface that may stay pinned to local traps. From field theory studies, such a behavior is denoted *multiplicative noise* (MN) and is equivalent to the behavior of the (bounded) Kardar-Parisi-Zhang equation, which describes the behavior of a growing surface that tends to pin and is pushed from below [10–14]. On the other hand, stable systems have a negative MLE. So, replicas should naturally synchronize once their distance is (locally) below the threshold of validity of linear analysis. However, when the (local) difference is large, nonlinear terms may maintain or amplify this distance. In this case synchronized patches may be destabilized only at the boundaries. Again, theoretical studies associate such a behavior to that of directed percolation (DP) [7,15,16]. In other words, one may illustrate this behavior by saying that the synchronized state is similar to the *void* state of the field theory descriptions, and that this void state is absorbing in the second case and unstable in the first case [17].

It has been noted that CMLs with continuous chaotic maps lead to synchronization with a MN character while the synchronization of CMLs where the local map is discontinuous [7,18], or with very sharp transitions [8], belong to the DP universality class. The use of simple models where the transition between the two behaviors may be triggered by a variation of control parameter has been addressed for the stochastic synchronization of CMLs in Ref. [16] and in growth models in Refs. [13,14]. Randomness can be safely used if the system is chaotic although the systems under
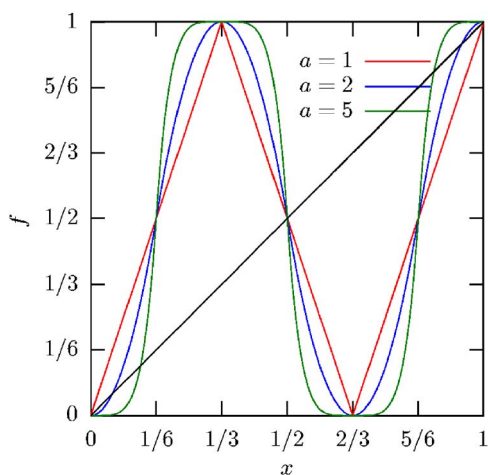
FIG. 1. (Color online) The graph of $f(x)$ for three values of a.

study are deterministic. This is not the case when there is stable chaos, unless coarse graining is used.

In what follows we investigate the relation between stability and the synchronization character of CMLs. We present a model that, by changing continuously a single parameter, can vary smoothly from *chaotic* to *chaotically stable* (nonchaotic but unpredictable) behavior, and finally to *cellular automata* behavior. From the point of view of the synchronization transition, the model exhibits a transition from the MN universality class to that of DP. The transition from chaos to stable chaos occurs at the same value of the parameter as the transition from the MN to the DP universality class. Moreover, we show that these transitions occur for smooth and continuous maps, and that at the transition stable synchronized trajectories are still present. The transition from standard chaos to stable chaos occurs through the appearance of transient chaos, i.e., the system in the stable chaotic phase exhibits a transient chaotic behavior before being attracted into the stable-chaos trajectory.

The paper is organized as follows. In Sec. II we present the CML model and the synchronization mechanism. In Sec. III we present the main numerical results, which we discuss in Sec. IV, and in Sec. V we end with some conclusions and directions for further work.

II. THE MODEL

A coupled map lattice F defines a flow on $[0,1]^N$, $\mathbf{x}^{t+1} = F(\mathbf{x}^t)$ with $\mathbf{x} = (x_0, \ldots, x_{N-1})$ and $t = 0, 1, \ldots$. It is defined locally by

$$x_i^{t+1} = f((1 - 2\epsilon)x_i^t + \epsilon(x_{i-1}^t + x_{i+1}^t)), \qquad (1)$$

with $i = 0, \ldots, N-1$ and periodic boundary conditions, $0 \le \epsilon \le 1/2$ and $f:[0,1] \to [0,1]$. In what follows, $\epsilon = 1/3$ so that

$$x_i^{t+1} = f(\sigma_i^t), \qquad (2)$$

with $\sigma_i = (x_{i-1} + x_i + x_{i+1})/3$.

The model is defined by the choice of f that depends on a parameter a such that for large values of this parameter, the
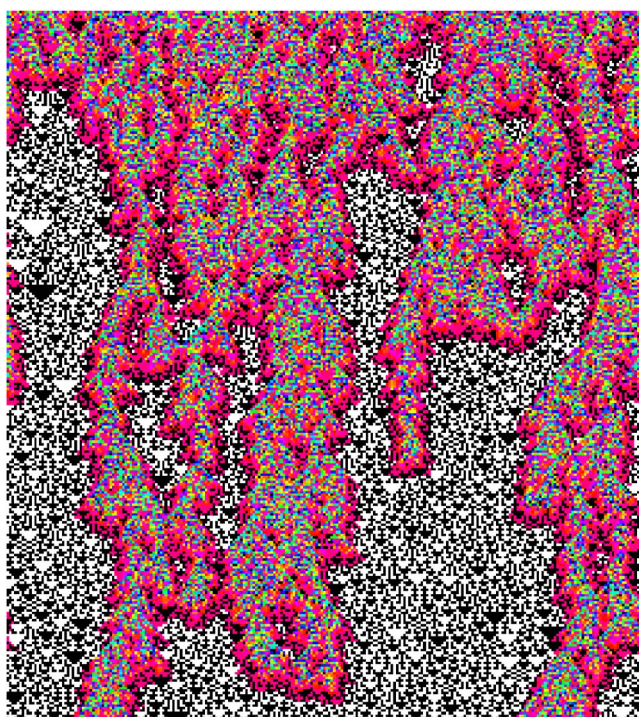

FIG. 2. (Color online) Space time pattern of the CML of Eq. (2) with $a = 1.9$ and $N = 256$ drawn horizontally for a total of $T = 300$ time steps drawn vertically from top to bottom. The initial configuration $\mathbf{x}^0$ is chosen randomly. The color code assigns white (black) whenever $x_i^t = 0(1)$ and a rainbow color scale for other values of x_i^t starting with red for values near zero. Patches of CA behavior (rule 150) appear after a short transient and will eventually fill the whole pattern.

CML behaves as an elementary cellular automaton (superstable system), and in the other limit the individual map is chaotic. One way to define f is by

$$f(x;a) = \begin{cases} (6x)^a/2 & 0 \le x < 1/6, \\ 1 - |6(1/3 - x)|^a/2 & 1/3 \le x < 1/2, \\ |6(x - 2/3)|^a/2 & 1/2 \le x < 5/6, \\ 1 - [6(1 - x)]^a/2 & 5/6 \le x < 1, \end{cases} \qquad (3)$$

where $1 \le a < \infty$. This function was introduced in Ref. [19] in the context of stochastic synchronization.

The graph of f is shown in Fig. 1 and a typical space time pattern is shown in Fig. 2. For a choice of the parameter $a \gtrsim 1.8$, the CML is asymptotically equivalent to a cellular automaton (CA) with triangles of 0 and 1. The function f was chosen in such a way that the CML in the limit of large a will behave as the "chaotic" elementary CA rule 150 [1].

Chaotic systems are characterized by the divergence of initially near trajectories, and a quantitative indicator for chaotic motion is (generally) a positive maximum Lyapunov exponent (MLE) $\lambda(\mathbf{x}^0)$, that depends on the trajectory. In order to probe the configuration space, we numerically evaluate $\lambda_{M,T}$, the average over M initial randomly chosen configurations $\mathbf{x}^0$ of finite-time Lyapunov exponents during T time steps.
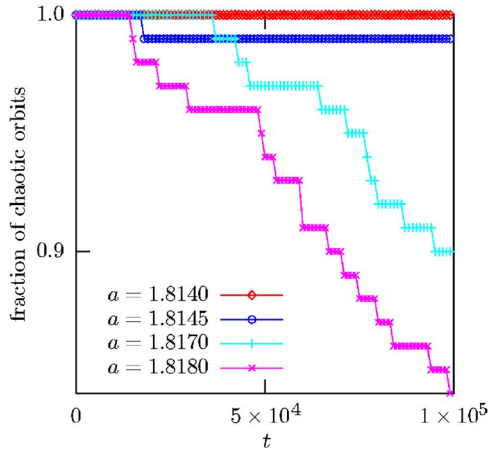
FIG. 3. (Color online) Fraction of chaotic orbits as a function of time for different values of a for a total of $M=100$ random initial states, $N=1024$ and $T=100N$.

We study the synchronization of CMLs by considering the following scheme:

$$x_i^{t+1} = f(\sigma_i^t), \tag{4}$$

$$y_i^{t+1} = (1-p)f(\tau_i^t) + pf(\sigma_i^t), \tag{5}$$

$$u_i^{t+1} = |x_i^{t+1} - y_i^{t+1}| \tag{6}$$

$$= (1-p)|f(\sigma_i^t) - f(\tau_i^t)|, \tag{7}$$

where $\tau_i = (y_{i-1} + y_i + y_{i+1})/3$. Synchronization occurs when $u_i^t \to 0 \, \forall i$, which is equivalent to a vanishing norm u^t of $\mathbf{u}^t$ defined by

$$u^t = \frac{1}{N}\sum_i u_i^t. \tag{8}$$

The synchronization threshold is called p_s. In numerical simulations, we usually evaluate $\langle u \rangle$, defined as an average over T time steps after a relaxation time t_{rel} which is then averaged over M random initial conditions. In Fig. 6 we show u^t for several values of a and p_s.

The linear stability of u is measured by the transverse Lyapunov exponent (TLE) $\lambda_\perp$ defined by [20]

$$\lambda_\perp(\mathbf{x}^0) = \ln(1-p) + \lambda(\mathbf{x}^0). \tag{9}$$

The synchronized state becomes stable with respect to infinitesimal perturbation when $\lambda_\perp = 0$ so that the value of p at synchronization, p_ℓ, is given in the linear approximation by

$$p_\ell = 1 - \exp(-\lambda). \tag{10}$$

This does not mean that synchronization actually takes place for this value of p. It may happen that the system stays unsynchronized for $p > p_\ell$. In Ref. [7] this behavior has been associated with discontinuities of the single map, taking as reference the Bernoulli shift. We shall show in the following that even smooth, nonchaotic maps may correspond to $p_s > p_\ell$.

III. RESULTS

We first discuss the stability properties of the CML presented in the previous section and then the character of the synchronization transition. If $1 < a < a_c$ the CML is chaotic and if $a > a_c$ the CML exhibits stable chaos. We found $a_c = 1.8142(2)$ as discussed below. For $1 < a < a_c$ almost any trajectory starting at any initial state $\mathbf{x}^0$ with x_i^0 chosen randomly between 0 and 1 has a positive MLE. However, if the initial state is such that $x_i^0 = 0, 1$ randomly, the CML will evolve as the elementary CA rule 150 with a negative MLE (actually $\lambda = -\infty$).

The configuration space of the system is the unitary hypercube $[0,1]^N$, whose vertices correspond to automata configurations (0 and 1). Starting from one vertex, the time evolution will visit only vertices. There is an attractor near the vertices of the hypercube that brings any trajectory with initial state in this attractor toward these CA trajectories. The transition from chaos to stable chaos corresponds to the transition where this attractor fills the hypercube.

For $a > a_c$ the system exhibits transient chaos: initially nearby trajectories diverge and are finally attracted to a CA-type evolution. Numerically one observes a positive finite-time MLE that (suddenly) becomes negative. This fact is used to find the value of a_c as shown in Fig. 3. For different values of a, the MLE of M orbits starting from randomly chosen initial states is evaluated and the fraction of chaotic orbits is shown as a function of time. The first value of a for which this fraction is not one is taken as a_c. For $a > a_c$ the fraction of chaotic orbits goes to zero as $t \to \infty$ so the measure of the set of initial states showing stable chaos goes to one.

Let us now turn to synchronization. In Fig. 4 we show the dependence of the order parameter $\langle u \rangle$ with p. For values of a close to the critical value there is a wide spread in the values of u as shown in Fig. 4(b) making it difficult to define p_s. By letting the system to relax longer, we find a well-defined synchronization threshold as shown in the inset of the figure. In Fig. 5 we show the phase diagram of p_s vs a. Note the large jump of p_s at a_c.

For $a < a_c$, $p_s \simeq 0.5$ and for values of p close to this value, the two replicas are forced to stay a small distance apart, so that only the linear (chaotic) separation is active. The synchronization transition thus occurs in agreement with Eq. (10), the difference field may be contracting or expanding, according with p, but the synchronized state is not absorbing [Fig. 6(a)]. By increasing a, the Lyapunov exponent drops to $-\infty$ [Fig. 6(b)] and we cross the phase boundary. By lowering p, the nonlinear mechanism for the diffusion of the difference field is activated and sustains the differences between the replicas. The cluster of nonsynchronized sites is now connected, such as in DP clusters [Fig. 6(c)]. By further increasing a, the linear mechanism becomes quickly contracting, and the nonsynchronized cluster is more reminiscent of cellular automata ones [Fig. 6(d)].

By extensive numerical simulations we found the values of the critical exponents δ, β, and z defined by

$$\langle u \rangle \sim (p_s - p)^\beta, \quad \langle u^t \rangle \sim t^{-\delta}, \quad \langle u^t \rangle \sim N^{-\delta z}g(tN^{-z}),$$

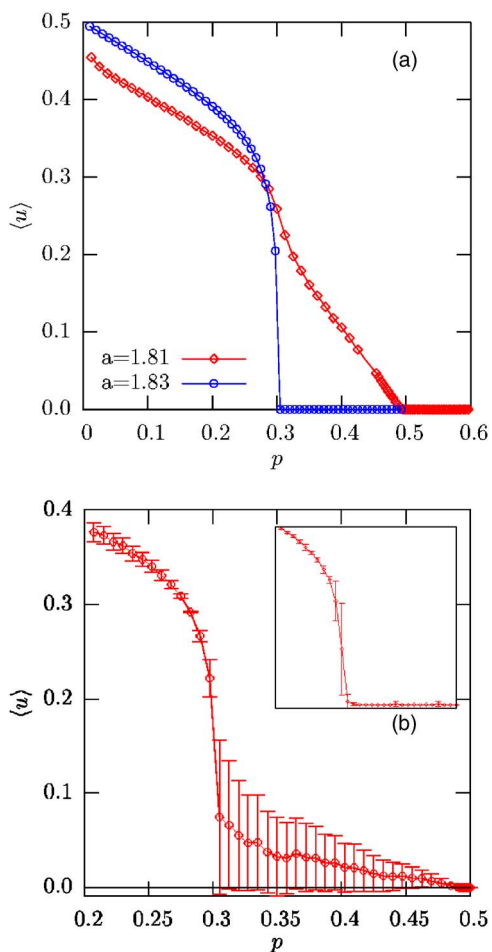with g an unknown function. For a below the critical value a_c the synchronization transition belongs to the bounded

FIG. 5. (Color online) Synchronization threshold p_s vs a. Labels refer to patterns in Fig. 6.

IV. DISCUSSION

Our results suggest that the jump from one universality class to the other occurs at the value a_c where the jump from chaos to stable chaos occurs. In other words, the microscopic stability properties of the CML are responsible for its macroscopic synchronization transition.

Near the synchronization threshold, the difference field behavior is dominated by the spreading properties of nonsynchronized patches, which is exactly what is generally measured for the determination of the critical properties of the transition. The evolution of the difference field, which is in average small at the transition, is related to the linear stability of the individual map: systems which are linearly expanding (positive MLE) exhibit a difference field which is locally small everywhere, with occasional fluctuations. In this case one has a local competition between the synchronization strength and the diverging character of the dynamics. Systems exhibiting stable chaos, however, are quite different. The difference field cannot be small, otherwise it would spontaneously vanish due to the negativity of MLE. Therefore, it has to be large in some patches of small extension (since at the transition it is small in average), and is maintained and propagated by the nonlinear part of the dynamics that amplifies "instantaneously" the differences between replicas. This amplification means that even if two state values in a certain location of the two replicas are similar, they may become very different in just one step. This effect can obviously be generated by the explicit discontinuities in the local evolution rule [7], but may manifest also in continuous maps, as shown by our toy model. Actually, our model exhibits this behavior when the dynamics has reached the "cellular automaton phase," i.e., after the eventual transient chaotic regime. In this CA phase the effective dynamics is discontinuous, but this behavior is not easily recognizable just by looking at the local evolution rule. Notice that DP-like transition can be exhibited also by truly chaotic systems with discontinuities, like Bernoulli shifts [7]. Our results are consistent with recent findings using a stochastic field theory

FIG. 4. (Color online) Dependence of the order parameter $\langle u \rangle$ on p near the critical value a_c. In (a) $T = t_{rel} = 5 \times 10^4$, $M = 100$, and $N = 1024$. In (b) the standard deviation is rather large for the same values of T, t_{rel}, M, and N making it difficult to assign a value to p_s. However, by making $t_{rel} = 10^5$ there is a well-defined transition at $p_s = 0.303$ as shown in the inset.

Kardar–Parisi–Zhang (BKPZ) universality class ($\delta = 1.10 \pm 0.12$, $\beta = 1.5 \pm 0.15$, and $z = 1.53 \pm 0.07$) and for $a > a_c$ it belongs to the directed percolation (DP) universality class [$\delta = 0.159464(6)$, $\beta = 0.276486(6)$, and $z = 1.580745(1)$ as shown in Fig. 7]. The precision of the reference values of the critical exponents reflect the difficulties in measuring the critical behavior of systems in the presence (absence) of absorbing states. Numerical experiments concerning DP are much more precise that those concerning MN, due to the absorbing character of the void state. In both cases the most sensitive measure concerns the spreading rate of a defect, but while in some DP simulations (not in this case) it is sufficient to simulate the behavior of the system around the spreading damage (the evolution of the void state is trivial), in MN experiments one has to simulate the whole system. This implies that these DP experiments immediately reach the asymptotic limit for what concerns the spatial dimension, while MN experiments suffer from finite-size spatial effects. Moreover, DP systems may be discrete, while MN ones are simulated using floating-point arithmetic.
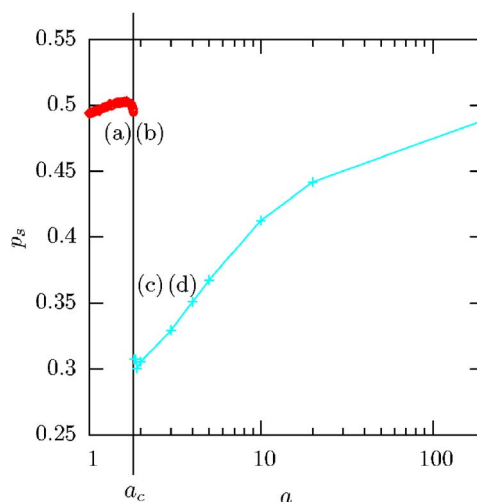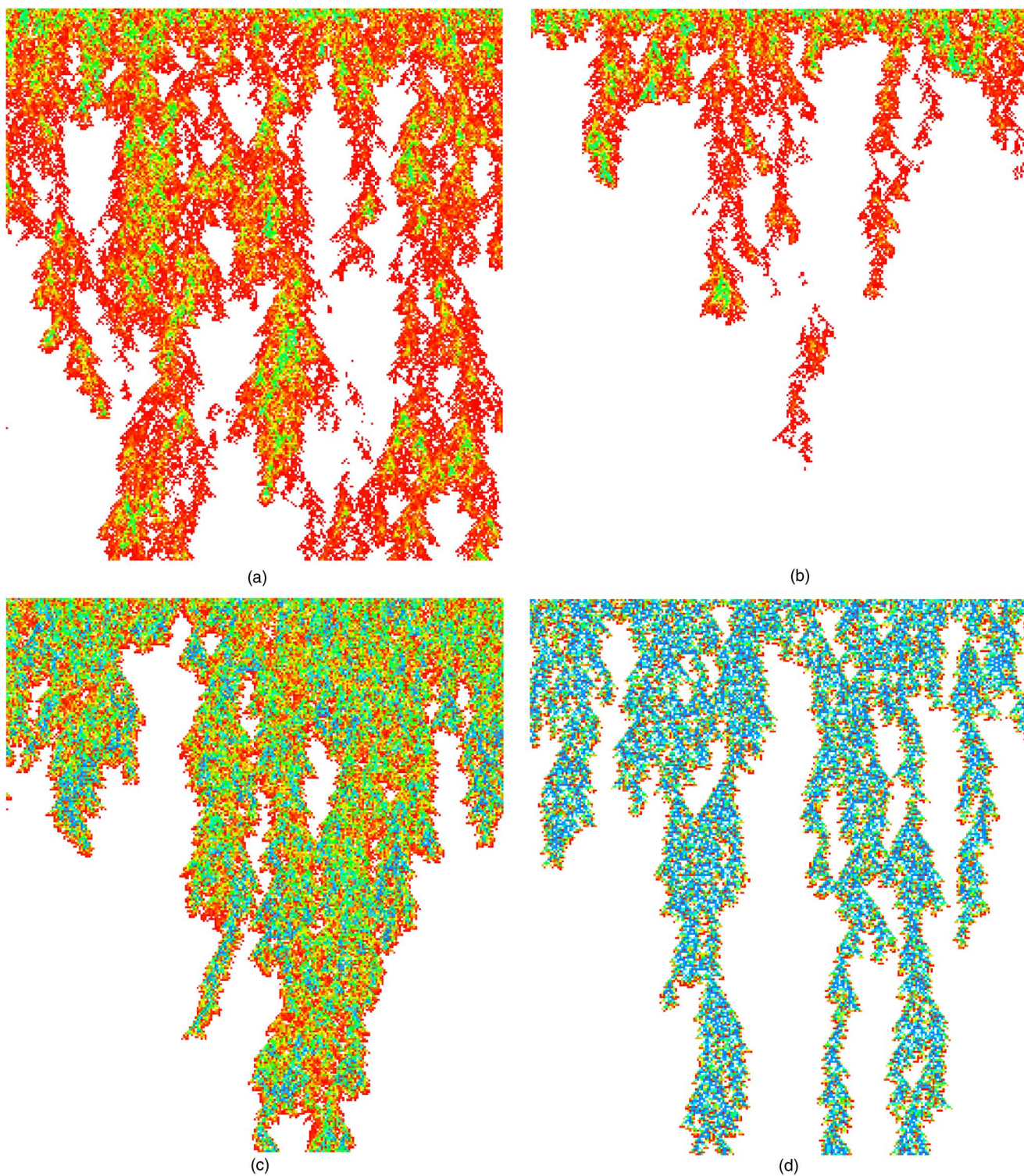
FIG. 6. (Color online) Synchronization space time patterns near p_s for different values of a. See Fig. 5 for reference. (a) $a=1.8$ $<a_c(\lambda>0)$, $p=0.48<p_s(1.8)$: the difference field is expanding but low in value, and the synchronized state is not locally absorbing (b) $a=1.9>a_c(\lambda<0)$, $p=0.48\geqslant p_s(1.9)$: the difference field is contracting, and the synchronized state is absorbing, even though occasionally patches of nonsynchronized sites appear. (c) $a=1.9>a_c$, $p=0.36\geqslant p_s(1.9)$: the difference field is sustained by the nonlinear term, the unsynchronized sites form a connected cluster. (d) $a=3.5\gg a_c$, $p=0.36\geqslant p_s(3.5)$: the linear contribution to the difference field is (almost) absent, the nonsynchronized cluster is connected and has more "holes" than in case (c). $N=256$, $T=256$
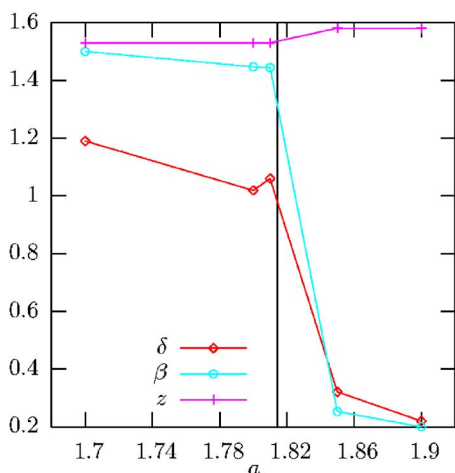
FIG. 7. (Color online) The values of the critical exponents δ, β, and z for different values of a. The vertical line is drawn at a_c = 1.8142.

that recovers both MN and DP behavior in a unified way related to the change of stability of the system [17].

V. CONCLUSIONS

We have investigated the relation between the type of unpredictability and synchronization transition universality classes, using a coupled map lattice model where the local dynamics is given by a continuous map that can exhibit chaotic or stable character. This model may exhibit either chaotic unpredictability or stable chaos.

We have analyzed the synchronization properties of two replicas, coupled asymmetrically with a parameter p. Linear stability analysis gives an estimate synchronization threshold p_ℓ related to λ. This is actually the case for smooth chaotic maps.

We have shown that this *transverse* direction may stay expanding (i.e., the system does not synchronize) for $p > p_\ell$. In this case the synchronized trajectories are actually absorbing, but the measure of initial conditions that bring toward them is vanishing.

We expect to observe similar behavior in other, more physical systems, and in particular in biological ones: the kind of unpredictability (chaos) observed in biological systems cannot be ascribed to a chaotic behavior of cells, that in viable conditions are rather stable unities, but is presumably due to the coupling among them, in a way that is reminescent of cellular automata "chaos."

Actually, cellular automata have become a widely adopted modeling tool, due to the simplicity of description of the interaction rules and the efficient simulating techniques. They have been used to model a wide variety of systems, from physics to engineering to biology. However, one may ask where is the transition from the continuous, microscopic world to the discrete, macroscopic description of cellular automata. This is exactly the question addressed in this paper, and we have shown an example in which this transition may be located quite precisely.

[1] S. Wolfram, Rev. Mod. Phys. **55**, 601 (1983).

[2] A. Politi, R. Livi, G.-L. Oppo, and R. Kapral, Europhys. Lett. **22**, 571, (1993).

[3] F. Cecconi, R. Livi, and A. Politi, Phys. Rev. E **57** 2703 (1998),

[4] J. P. Crutchfield and K. Kaneko, Phys. Rev. Lett. **60**, 2715 (1988); K. Kaneko, Phys. Lett. A **149**, 105 (1990).

[5] L. M. Pecora and T. L. Carroll, Phys. Rev. Lett. **64**, 821 (1990).

[6] M. Rosenblum, J. Kurths, and A. Pikovsky, *Synchronization: A Universal Concept in Nonlinear Sciences* (Cambridge University Press, Cambridge, England, 2001).

[7] V. Ahlers and A. Pikovsky, Phys. Rev. Lett. **88** 254101 (2002).

[8] M. Droz and A. Lipowski, Phys. Rev. E **67**, 056204 (2003).

[9] L. Baroni, R. Livi, and A. Torcini, Phys. Rev. E **63**, 036226 (2001).

[10] M. Kardar, G. Parisi, Y. C. Zhang, Phys. Rev. Lett. **56**, 889 (1986).

[11] A. Schenzle and H. Brand, Phys. Rev. A **20**, 1628 (1979); W. Horstemke and R. Lefever, *Noise Induced Transitions* (Springer, Berlin, 1984); C. Van den Broeck, J. M. R. Parrondo, J. Armero, and A. Hernandez-Machado, Phys. Rev. E **49**, 2639 (1994); C. Van den Broeck, J. M. R. Parrondo, and R. Toral, Phys. Rev. Lett. **73**, 3395 (1994).

[12] G. Grinstein, M. A. Muñoz, and Y. Tu, Phys. Rev. Lett. **76**, 4376, (1996); Y. Tu, G. Grinstein, and M. A. Muñoz, *ibid.* **78**, 274 (1997).

[13] F. Ginelli, V. Ahlers, R. Livi, D. Mukamel, A. Pikovsky, A. Politi, and A. Torcini, Phys. Rev. E **68**, 065102(R) (2003).

[14] A. Lipowski and M. Droz, Phys. Rev. E **68**, 056119 (2003).

[15] P. Grassberger, Phys. Rev. E **59**, R2520 (1999).

[16] F. Ginelli, R. Livi, A. Politi, and A. Torcini, Phys. Rev. E **67**, 046217 (2003).

[17] M. A. Muñoz and R. Pastor-Satorras, Phys. Rev. Lett. **90**, 204101 (2003).

[18] P. Grassberger, Phys. Rev. E **59**, R2520 (1999).

[19] F. Bagnoli and F. Cecconi, Phys. Lett. A **260**, 9 (2001).

[20] L. M. Pecora and T. L. Carroll, Phys. Rev. Lett. **64**, 821 (1990); Phys. Rev. A **44**, 2374 (1991).